Melting Experiments on the Enstatite-Pyrope Join at 80–152 kbar

Tibor Gasparik

Center for High Pressure Research, Department of Earth and Space Sciences
State University of New York at Stony Brook

Melting temperatures of the assemblage pyroxene + garnet on the enstatite-pyrope join were experimentally determined at 11 different pressures between 80 and 152 kbar with a split-sphere anvil apparatus (USSA-2000). The compositions of pyroxene, garnet, and melt coexisting along the solidus were also determined. Comparison with previous data at lower temperatures revealed a large temperature dependence of the compositions of garnet coexisting with pyroxene. It is proposed that the observed variation in the garnet composition is caused by disorder in garnet. The obtained alumina contents of orthopyroxene coexisting with garnet on the solidus at 80–110 kbar contributed to an improvement of the garnet peridotite thermobarometry. An internally consistent set of thermodynamic parameters was derived, which allows calculation of the temperature-pressure phase diagram for the enstatite-pyrope join at 20–260 kbar.

Introduction

The three-component chemical system MgO-Al_2O_3-SiO_2 (MAS) accounts for 90% of Earth's mantle; the bulk composition of the mantle falls within the subsystem enstatite-pyrope-forsterite ($Mg_2Si_2O_6$-$Mg_3Al_2Si_3O_{12}$-Mg_2SiO_4). The compositions of coexisting pyroxene and garnet on the enstatite-pyrope join are primarily pressure dependent and thus suitable for the geobarometry of mantle xenoliths. Phase relations in the MAS system are fundamental for understanding the mineralogy of the mantle; the addition of other elements modifies, but does not qualitatively alter, these phase relations. The importance of the MAS system was recognized early, as reflected in a large number of experimental studies carried out in this system. Most of these studies were done with a piston and cylinder apparatus and thus are limited to pressures below 50 kbar. Recent studies with multianvil devices allowed us to extend the phase relations to pressures above 200 kbar. This study provides new data for the enstatite-pyrope join at these high pressures and at the solidus temperatures, which were necessary to complete the phase diagram for this join.

Experimental Techniques

Experiments were carried out with a split-sphere anvil apparatus using the 10-mm sample assembly designed by *Gasparik* [1989]. The sample enclosed in a rhenium container was placed in the assembly slightly off-center, so that the hot spot was at the end of the sample. Temperature was measured by W3%Re versus W25%Re axial thermocouples and estimated using the 1-bar calibration of the emf versus temperature. The nominal temperature measured and controlled by the thermocouple was approximately in the center of the sample. The temperature increase between the center and the hot spot was approximately 50°C; the temperature drop between the hot spot and the cold end of the sample was about 200°C. The description of the apparatus and the sample assembly, the temperature and pressure calibrations, and the experimental procedures are given by *Gasparik*

[1989]. Temperatures were reproducible within 30°C and pressures within 3 kbar.

Starting materials were mechanical mixes of high purity SiO_2, MgO, and synthetic $MgAl_2O_4$ spinel (Table 1). Experimental products were mounted in epoxy for microprobe analysis; a polished mount contained a lengthwise section of the whole sample inside of a rhenium container. Wavelength dispersive chemical analyses were obtained with a Cameca electron microprobe.

Experimental Results

Melting temperatures (in degrees Celsius) of the assemblage pyroxene + garnet were determined at 11 different pressures between 80 and 152 kbar (2030/80, 2060/90, 2100/100, 2140/110, 2190/121, 2220/126, 2230/130, 2260/135, 2280/140, 2280/146, 2280/152), and the compositions of coexisting pyroxene, garnet, and liquid (present as quenched crystals) are listed in Table 1 and shown in Figure 1.

In most of the experiments the solidus was located in the hot spot of the samples. Because of the small temperature gradients in the hot spot this location yields the most reliable estimate of the melting temperatures. The solidus has a pronounced inflection between 140 kbar and the triple point for coexisting clinoenstatite, majorite, and liquid, located at 2335°C and 164 kbar by *Presnall and Gasparik* [1989]. This inflection, which is even more pronounced on the enstatite-jadeite join [*Gasparik*, 1992], is likely caused by azeotropic melting of highly majoritic garnets (70–90% majorite).

In most of the experiments the liquid was multiply saturated with pyroxene and garnet; thus the liquid compositions are good approximations of the eutectic compositions. The eutectic compositions are much closer to enstatite than pyrope (Figure 1). The pyroxene compositions show a clear discontinuity at the orthopyroxene–clinopyroxene transition. The observed range of the clinopyroxene compositions is very narrow at all pressures. The range of the orthopyroxene compositions is narrow only at 110 kbar and widens at lower pressures. This apparently reflects the well-known tendency for orthopyroxene to acquire metastable alumina contents in synthesis experiments that are higher than the stable contents. The orthopyroxene composition at 110 kbar provides the best estimate of the alumina content of orthopyroxene coexisting with garnet at these high pressures and in

Table 1. Experimental Conditions and Average Compositions of Phases

Run	Mix[a]	t^b, min	P_g^c, bars	P_s^d, kbar	T_s^e, °C	Phase[f]	Number of Analyses[g]	Cations/Six Oxygens			
								Mg	Al	Si	Sum
1219	A	6	114	80	2050	L	8	1.876	0.270	1.859	4.005
					2030	Px	12	1.948	0.122	1.935	4.005
					2030	Ga	6	1.565	0.923	1.525	4.013
1208	A	4	135	90	2060	L	14	1.849	0.247	1.890	3.986
					2060	Px	12	1.951	0.091	1.957	3.999
					2060	Ga	19	1.582	0.855	1.568	4.005
1214	A	6	160	100	2100	L	6	1.837	0.205	1.928	3.970
					2100	Px	18	1.956	0.073	1.968	3.997
					2100	Ga	23	1.617	0.796	1.595	4.008
1203	B	6	160	100	2100	L	12	1.894	0.144	1.945	3.983
					2100	Px	11	1.957	0.077	1.964	3.998
					2100	Ga	6	1.613	0.787	1.603	4.003
1197	B	6	190	110	2150	L	7	1.945	0.109	1.946	4.000
					2140	Px	10	1.973	0.055	1.972	4.000
					2140	Ga	6	1.656	0.700	1.647	4.003
1195	B	6	230	121	2200	L	6	1.943	0.099	1.955	3.997
					2190	Ga	14	1.741	0.551	1.716	4.008
					2180	Px	9	1.991	0.020	1.990	4.001
1215	B	4	250	126	2220	L	9	1.954	0.049	1.986	3.989
					2220	Px	8	1.987	0.017	1.994	3.998
					2220	Ga	19	1.743	0.515	1.742	4.000
1191	B	6	270	130	2250	L	8	1.953	0.113	1.938	4.004
					2230	L	9	1.984	0.058	1.965	4.007
					2230	Px	5	1.985	0.015	1.996	3.996
					2230	Ga	20	1.777	0.474	1.756	4.007
1174	C	6	295	135	2300	L	11	1.886	0.103	1.980	3.969
					2260	L	23	1.968	0.048	1.980	3.996
					2260	Px	10	2.004	0.013	1.988	4.005
					2250	Ga	13	1.827	0.389	1.795	4.011
1180	C	6	320	140	2300	L	25	1.969	0.029	1.994	3.992
					2280	Px	12	1.994	0.012	1.994	4.000
					2280	Ga	10	1.837	0.326	1.837	4.000
1184	C	6	360	146	2340	L	5	1.952	0.068	1.973	3.993
					2280	L	8	1.978	0.029	1.989	3.996
					2280	Px	9	2.006	0.007	1.991	4.004
					2280	Ga	31	1.875	0.266	1.863	4.004
1186	C	6	400	152	2300	L	7	1.994	0.032	1.979	4.005
					2280	Ga	27	1.906	0.197	1.900	4.003
					2270	Px	5	2.014	0.006	1.988	4.008

[a] A, 1.8 mol SiO_2, 1.6 MgO, 0.2 $MgAl_2O_4$; B, 1.9 SiO_2, 1.8 MgO, 0.1 $MgAl_2O_4$; C, 1.95 SiO_2, 1.9 MgO, 0.05 $MgAl_2O_4$.
[b] Duration of experiments.
[c] Gauge pressure ($\times$ 1.096 is load in metric tons).
[d] Sample pressure.
[e] Sample temperature in the hot spot (nominal T + 50°C) and at lower temperatures.
[f] L, liquid; Px, pyroxene; Ga, garnet.
[g] The total number of analyses accepted from the given experiment for each phase.

combination with the low-pressure data narrowly constrains the position of the pyroxene isopleths in the T-P plane.

The pyroxene content of garnet increases almost linearly with pressure. This is in sharp contrast with the previous data at 1000°–1650°C [*Ringwood*, 1967; *Akaogi and Akimoto*, 1977; *Liu*, 1977; *Kanzaki*, 1987; *Gasparik*, 1989] that show, in general, a slow increase in the pyroxene content of garnet over a large pressure range at pyrope contents greater than 50% but a much faster increase over a narrow pressure range at higher pyroxene contents. Comparison with the 1650°C data of *Gasparik* [1989], shown in Figure 1, reveals a large temperature dependence of the garnet compositions, which can only be explained by increasing disorder of magnesium, silicon, and aluminum in the octahedral site of garnet. It is very likely that the garnet along the enstatite-pyrope solidus is close to being completely disordered.

EVIDENCE OF DISORDER IN ENSTATITE-PYROPE GARNET

The observed large temperature dependence of the compositions of enstatite-pyrope garnet coexisting with pyroxene is only one example of the strong effect of disorder in majorite (pyroxene-rich) garnets on phase relations. This effect is even more pronounced in the enstatite-jadeite garnets [*Gasparik*, 1989, 1992] and was also observed in the enstatite-diopside and enstatite-NaPx ($Na_2MgSi_5O_{12}$) garnets [*Gasparik*, 1989; *Herzberg and Gasparik*, 1991]. The observed difference in the enstatite-pyrope garnet compositions between 1650°C and the solidus temperatures is comparable to the difference obtained theoretically between an ideal completely ordered ($a_{Py} = X_{Py}$) and completely disordered ($a_{Py} = X_{Py}^2$) garnet solution [*Gasparik*, 1989]. Thus the enstatite-pyrope garnet should exhibit a large degree of order
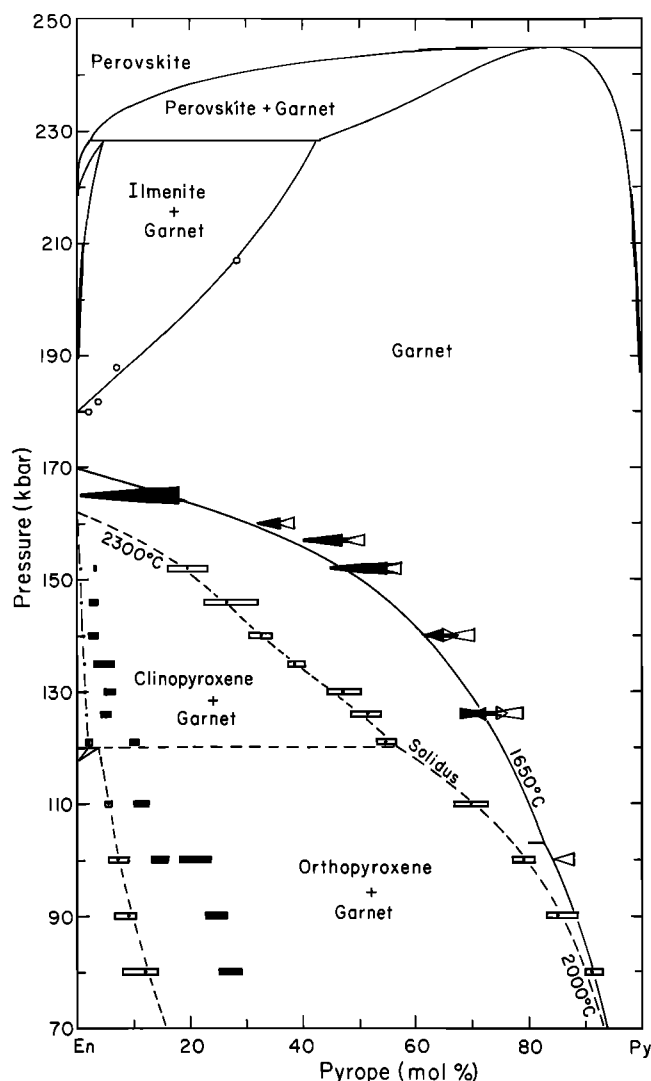
Fig. 1. Pressure-composition phase diagram for the enstatite-pyrope join at 1650°C (solid curves) and the solidus temperatures (dashed curves). Bars indicate the range of the observed compositions of liquid (solid symbols) and coexisting pyroxene and garnet (open symbols), with the average compositions indicated by dots. Solid arrows and circles are the data at 1650°C and open arrows at 1450°C from Gasparik [1989].

at temperatures below 1650°C. This contradicts the infrared, Raman and nmr study of McMillan et al. [1989], who found that intermediate enstatite-pyrope garnets were disordered. However, these garnets were synthesized from high-energy glasses at 900°–1000°C temperatures and would likely be metastably disordered. At such low temperatures, any equilibration of the garnet produced at the beginning of an experiment would be kinetically prohibited.

The large temperature dependence of disorder in more complex garnet solutions points to the possibility of disorder in the end-member $Mg_4Si_4O_{12}$ majorite. In majorite the octahedral sites are occupied by magnesium and silicon. Majorite has a tetragonal symmetry resulting from ordering of magnesium and silicon in two different octahedral sites. Similar tetragonal garnets, for example, $CaGeO_3$ and $CdGeO_3$, are completely ordered [Prewitt and Sleight, 1969]. The first structure determination of majorite synthesized at

1800°C indicated 40% disorder [Angel et al., 1989], although the structure determination was hampered by the poor quality of the crystals and pervasive twinning. The twinning was interpreted to arise because of cation ordering during crystal growth. In contrast, Hatch and Ghose [1989] argued that the twinning reflects a phase transition from cubic to tetragonal and formed during quenching. This would imply that majorite in its stability field is cubic. Howell et al. [1990] investigated cation ordering in majorite using ^{29}Si nmr spectroscopy and found that majorite synthesized at 2000°C was only 20% disordered. Wang et al. [1991] reported that majorite quenched from temperatures greater than 2400°C showed only modulated (tweed) microstructure, while majorite synthesized at lower temperatures showed also pseudo-merohedral twins indicative of a tetragonal symmetry. The lack of these twins at temperatures above 2400°C is consistent with a phase transition from cubic to tetragonal near 2400°C (at 226 kbar). This would imply that majorite at mantle conditions is tetragonal and thus at least partially ordered.

Gasparik [1990a] reinvestigated the phase relations in the system $MgSiO_3$, determined previously by Kato and Kumazawa [1985] and Sawamoto [1987], and found that the phase boundary between majorite and $MgSiO_3$ ilmenite is curved. He suggested that the curvature could either be caused by a large compressibility of majorite or due to disordering of majorite with increasing temperature. In view of the recent evidence for disorder in majorite, it is now proposed that this disorder is likely to be the dominant cause for the observed curvature of the majorite-ilmenite boundary. A more correct description of the boundary should include an excess heat capacity term arising from the disorder. In contrast, Gasparik [1990a] described the curvature solely with a pressure dependent term. Moreover, omission of this term in other equilibria with majorite introduced inconsistency which interfered with the calculation of phase diagrams.

To eliminate this inconsistency, new parameters were derived for all phase boundaries involving majorite using the following expression [Gasparik and Newton, 1984; Gasparik, 1990b]:

$$\Delta G_{T,P} = \Delta H° - T\Delta S° - cT^{1.2} + P\Delta V° - bP^2.$$

In this expression, b is a parameter expressing the differences in compressibilities, and c expresses the heat capacity differences arising from disorder. All units are in joules (J), kelvins (K), and bars (bars).

SUBSOLIDUS EQUILIBRIA IN THE SYSTEM $MgO-SiO_2$

The newly calculated phase relations for the enstatite-forsterite join are shown in Figure 2. The diagram closely reproduces the phase relations and experimental observations reported by Gasparik [1990a] and was calculated with an internally consistent set of parameters. The derivation of the parameters started by fitting the majorite-ilmenite and majorite to beta phase + stishovite boundaries.

Gasparik [1990a] synthesized ilmenite at 178 kbar and 1650°C, that is, at a much lower pressure than reported by Sawamoto [1987]. The majorite-ilmenite boundary was observed at 219 kbar and 2030°C. The majorite to beta phase + stishovite boundary was located at 175 kbar and 1600°C, which was at the same temperature as the projected triple
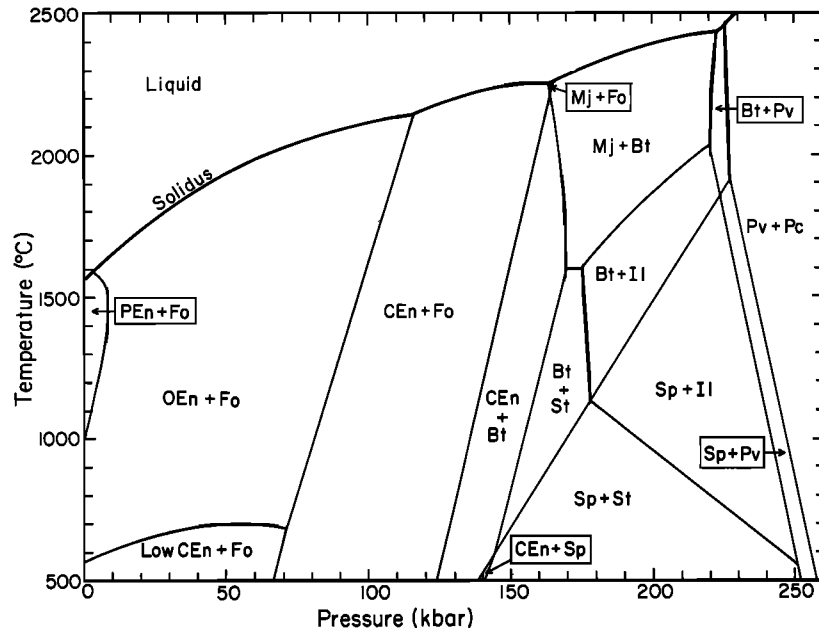
Fig. 2. Temperature-pressure phase diagram for the enstatite-forsterite join. Solidus is based on the works of *Chen and Presnall* [1975], *Presnall and Gasparik* [1990], and *Gasparik* [1990a].

point for coexisting clinoenstatite, majorite, beta phase, and stishovite. This indicated that the majorite to beta phase + stishovite boundary has a dP/dT slope close to infinity, which influenced the placement of the triple point for coexisting majorite, beta phase, stishovite, and ilmenite at 175.5 kbar and 1600°C. In the derivation of the parameters, constraints were imposed to keep the infinite slope of the majorite to beta phase + stishovite boundary and the original parameters from *Gasparik* [1990a] for the beta phase + stishovite to ilmenite boundary:

$$Mj = 4Il \qquad (1)$$

$$\Delta G(1) = 90,200 - 134.4T + 30T^{1.2} - (0.7 - 10^{-6}P)P$$

$$Bt + St = 2Il \qquad (2)$$

$$\Delta G(2) = 35,550 - 1.2T - 0.19P$$

$$Mj = 2Bt + 2St \qquad (3)$$

$$\Delta G(3) = \Delta G(1) - 2\Delta G(2)$$

$$\Delta G(3) = 19,100 - 132T + 30T^{1.2} - (0.32 - 10^{-6}P)P.$$

The clinoenstatite-majorite transition was observed by *Presnall and Gasparik* [1989] at 165 kbar and 2150°C, with enstatite at lower temperatures, while the clinoenstatite to beta phase + stishovite boundary was located at the same pressure and 1400°C, with clinoenstatite at higher temperatures. This was taken as evidence for a negative slope of the clinoenstatite-majorite boundary. These experimental observations were satisfied with the following parameters which place the triple point for coexisting clinoenstatite, majorite, beta phase, and stishovite at 170 kbar and 1600°C:

$$CEn = Bt + St \qquad (4)$$

$$\Delta G(4) = 61,000 + 12.8T - 0.5P$$

$$2CEn = Mj \qquad (5)$$

$$\Delta G(5) = 2\Delta G(4) - \Delta G(3)$$

$$\Delta G(5) = 102,900 + 157.6T - 30T^{1.2} - (0.68 + 10^{-6}P)P.$$

Gasparik [1990a] placed the triple point for coexisting majorite, ilmenite, and perovskite at 220 kbar and 2030°C and confirmed the positive slope of the majorite-perovskite transition, first proposed by *Sawamoto* [1987]. The ilmenite-perovskite transition was based on the study by *Ito and Takahashi* [1989]:

$$Il = Pv \qquad (6)$$

$$\Delta G(6) = 88,500 - 6.9T - 0.33P$$

$$Mj = 4Pv \qquad (7)$$

$$\Delta G(7) = \Delta G(1) + 4\Delta G(6)$$

$$\Delta G(7) = 444,200 - 162T + 30T^{1.2} - (2.02 - 10^{-6}P)P.$$

By retaining the original parameters for reaction (2), parameters for several other equilibria remain the same as given by *Gasparik* [1990a]:

$$Bt = Sp \qquad (8)$$

$$\Delta G(8) = 10,700 + 7.6T - 0.12P$$

$$Sp + St = 2Il \qquad (9)$$

$$\Delta G(9) = \Delta G(2) - \Delta G(8)$$

$$\Delta G(9) = 24,850 - 8.8T - 0.07P.$$

The breakdown of spinel to perovskite and periclase is based on the study by *Ito and Takahashi* [1989], and the original parameters were modified to be consistent with the enthalpy

difference between spinel and perovskite constrained by equilibria at lower pressures:

$$Sp = Pv + Pc \qquad (10)$$

$$\Delta G(10) = 129{,}000 - 10.0T - 0.47P$$

$$Bt = Pv + Pc \qquad (11)$$

$$\Delta G(11) = \Delta G(8) + \Delta G(10)$$

$$\Delta G(11) = 139{,}700 - 2.4T - 0.59P.$$

Parameters for the equilibrium between forsterite and beta phase remained the same, and are consistent with data by *Katsura and Ito* [1989] at 1200°–1600°C, with the location of the boundary at 165 kbar and 2240°C reported by *Presnall and Gasparik* [1990], and with the enthalpy measurements of *Akaogi et al.* [1984]:

$$Fo = Bt \qquad (12)$$

$$\Delta G(12) = 30{,}000 + 6.7T - 0.284P.$$

The orthoenstatite-clinoenstatite boundary was reversed by *Pacalo and Gasparik* [1990] at 900°–1700°C, and *Presnall and Gasparik* [1990] observed the boundary at 116 kbar and 2140°C. Thermodynamic analysis by *Pacalo and Gasparik* [1990] showed conclusively that clinoenstatite stable at high pressures and temperatures is a new high-pressure polymorph of enstatite, structurally distinct from low ($P2_1/c$) or high ($C2/c$) clinoenstatite, and named the new phase high-pressure clinoenstatite (CEn). New data in the enstatite-jadeite system [*Gasparik*, 1992] provided constraints on the volume change of the orthoenstatite − high-P clinoenstatite transition, resulting in the following parameters:

$$OEn = CEn \qquad (13)$$

$$\Delta G(13) = 7{,}450 + 5.6T - 0.18P.$$

Parameters for the equilibria involving protoenstatite and low clinoenstatite were given by *Gasparik* [1990b].

MIXING PROPERTIES OF GARNET ON THE ENSTATITE-PYROPE JOIN

The mixing properties of garnet were derived using primarily the compositions of garnet coexisting with pyroxene at 1650°C [*Gasparik*, 1990a] and at the solidus temperatures (this study, Figure 1). Additional constraints included the compositions of garnet coexisting with $MgSiO_3$ ilmenite reported by *Gasparik* [1990a]. Initially, the alumina content of the coexisting pyroxene was neglected; the final refinement includes minor corrections arising from the small content of alumina in pyroxene. The observed garnet compositions do not show a potential effect from the phase transition between the tetragonal and the cubic garnet; thus the garnet was approximated as a single solid solution. Pyroxenes were approximated as ideal solutions. The best fit gave the following parameters:

$$2CEn = Mj \qquad (5')$$

$$RT \ln a_{Mj} - 2RT \ln X_{CEn} + \Delta G(5) = 0$$

$$\Delta G(5) = 102{,}900 + 157.6T - 30T^{1.2} - (0.68 + 10^{-6}P)P$$

$$2OEn = Mj \qquad (14)$$

$$RT \ln a_{Mj} - 2RT \ln X_{OEn} + \Delta G(14) = 0$$

$$\Delta G(14) = \Delta G(5) + 2\Delta G(13)$$

$$\Delta G(14) = 117{,}800 + 168.8T - 30T^{1.2} - (1.04 + 10^{-6}P)P$$

$$RT \ln a_{Mj} = 2RT \ln X_{Mj} + (29{,}000 - 18T)X_{Py}^2$$

$$+ (-131{,}000 + 60T)(4X_{Py}^3 - 3X_{Py}^2).$$

Equilibria with ilmenite and perovskite were calculated using the approach outlined by *Gasparik* [1990a]. Ilmenite was treated as a solid solution of $MgSiO_3$ (MgIl) and Al_2O_3 (AlIl). In this case, the transformation of garnet to ilmenite is azeotropic, and the univariant transformation of the most stable garnet to ilmenite occurs at some intermediate garnet compositions. This transformation was placed at 240 kbar, 1000°C, in agreement with the data of *Kanzaki* [1987]. The corresponding equilibria and parameters are

$$Mj = 4MgIl \qquad (1')$$

$$4RT \ln a_{MgIl} - RT \ln a_{Mj} + \Delta G(1) = 0$$

$$\Delta G(1) = 90{,}200 - 134.4T + 30T^{1.2} - (0.7 - 10^{-6}P)P$$

$$Py = 3MgIl + AlIl \qquad (15)$$

$$3RT \ln a_{MgIl} + RT \ln a_{AlIl} - RT \ln a_{Py} + \Delta G(15) = 0$$

$$\Delta G(15) = 180{,}000 + 40T - 0.7P$$

$$RT \ln a_{MgIl} = RT \ln X_{MgIl} - 60{,}000X_{AlIl}^2$$

$$RT \ln a_{AlIl} = RT \ln X_{AlIl} - 60{,}000X_{MgIl}^2.$$

At temperatures above 1100°C, garnet transforms azeotropically into perovskite. In the absence of data, it was assumed that the $MgSiO_3$-Al_2O_3 (MgPv-AlPv) perovskite solution has the same nonideality as the ilmenite solution. The width of the ilmenite + perovskite stability field was set arbitrarily by increasing the enthalpy change of the Al_2O_3 ilmenite to perovskite transition with respect to $\Delta H(6)$ by 3 kJ:

$$AlIl = AlPv \qquad (16)$$

$$\Delta G(16) = 91{,}500 - 6.9T - 0.33P.$$

These parameters were used to calculate the phase boundaries in Figure 1 and the garnet isopleths in Figure 3.

PYROXENES ON THE ENSTATITE-PYROPE JOIN

Aluminous pyroxenes are fundamentally important for thermobarometry; thus the alumina content of pyroxenes has been the target of many experimental investigations. The most common application of these experimental results is in the thermobarometry of spinel peridotites and garnet peridotites. The compositions of orthopyroxene and high-P clinopyroxene can be approximated as solid solutions of corresponding enstatite (En-$Mg_2Si_2O_6$) and Mg-Tschermak (MgTs-$MgAl_2SiO_6$) end-members.

In the MAS system the spinel peridotite assemblage consists of orthopyroxene, forsterite, and $MgAl_2O_4$ spinel. The stability is limited to pressures below 20–30 kbar,
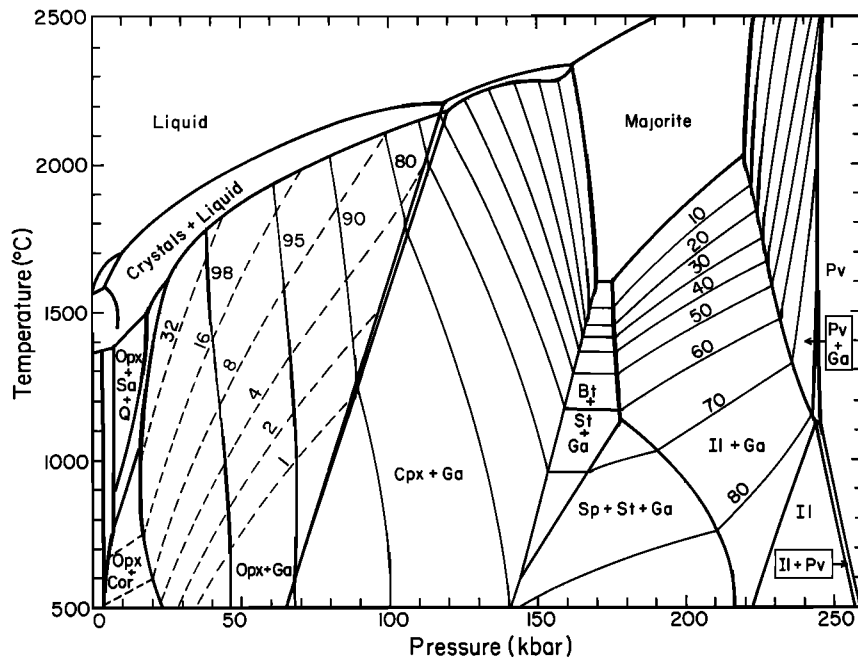
Fig. 3. Temperature-pressure phase diagram for the enstatite-pyrope join. Heavy curves are univariant boundaries and melting curves. Light solid curves are isopleths indicating the pyrope content of garnet (100 Al/6 oxygens), and light dashed curves are isopleths indicating the alumina content of orthopyroxene (100 Al/6 oxygens). The enstatite-pyrope solidus is based on this study and the data of *Boyd and England* [1964]. The liquidus corresponding to the melting curve of enstatite is based on the work by *Boyd et al.* [1964], *Gasparik* [1990b], and *Presnall and Gasparik* [1990]. Phase boundaries below 20 kbar are based on a work in preparation.

although at very low pressures, spinel is replaced with cordierite. At higher pressures, spinel peridotite is replaced with the garnet peridotite assemblage of orthopyroxene, pyrope and forsterite. The two divariant fields are separated by the univariant reaction:

$$2En_{(1-x)}MgTs_x + (1-2x)Sp = (1-2x)Fo + Py. \quad (17)$$
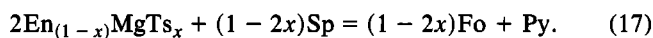
Gasparik and Newton [1984] calculated phase relations in the MAS system using their data in the spinel peridotite field, the data of *Perkins et al.* [1981] in the garnet peridotite field, and the position of the univariant curve (17) determined by reversals carried out with low-friction assemblies. Extrapolation of their isopleths in the garnet peridotite field to higher pressures does not give a satisfactory agreement with the present data; the isopleths underestimate the alumina content of orthopyroxene coexisting with garnet and thus the equilibration pressures in the geobarometry of garnet peridotites. The discrepancy resulted from the limited pressure range of the experiments by *Perkins et al.* [1981] that was insufficient to constrain the pressure dependence of the volume change for the corresponding equilibrium. This became possible with the data of *Herzberg and Gasparik* [1991], who reported the compositions of coexisting orthopyroxene, clinopyroxene, and garnet in the CMAS system at the solidus temperatures and 80–110 kbar pressures. The present data eliminated the uncertainty associated with the correction for the effect of calcium on the aluminum content of orthopyroxene.

The new parameters were derived assuming an ideal orthopyroxene solution of enstatite and Mg-Tschermak end-members, and using the experimental data in the spinel peridotite field of *Gasparik and Newton* [1984], the location

of the univariant curve (17) determined by *Danckwerth and Newton* [1978], *Haselton* [1979] and *Gasparik and Newton* [1984], and the present data at 80–110 kbar with a special emphasis on fitting the orthopyroxene composition at 110 kbar and 2140°C:

$$OEn + Sp = MgTs + Fo \quad (18)$$
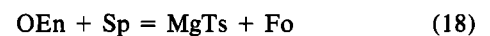
$$RT \ln X_{MgTs} - RT \ln X_{OEn} + \Delta G(18) = 0$$

$$\Delta G(18) = 23,400 - 2T$$

$$OEn + MgTs = Py \quad (19)$$

$$RT \ln a_{Py} - RT \ln X_{MgTs} - RT \ln X_{OEn} + \Delta G(19) = 0$$

$$\Delta G(19) = 8600 - 92.5T + 19T^{1.2} - (0.85 - 26 \times 10^{-7}P)P$$

$$RT \ln a_{Py} = 2RT \ln X_{Py} + (29,000 - 18T)X_{Mj}^2$$

$$+ (-131,000 + 60T)(3X_{Mj}^2 - 4X_{Mj}^3).$$

In most applications the majorite content of garnet is very low and can be neglected. The parameters were used to calculate the pyroxene isopleths in Figure 3.

COMPARISON WITH THERMOCHEMISTRY

The enthalpy, entropy, and volume differences derived above are internally consistent; thus it is possible to calculate from them the thermodynamic properties for each phase. The resulting parameters are shown in Table 2. A reference temperature of 970 K was chosen mainly to allow a direct comparison with the measured heats of solution that

Table 2. Thermodynamic Properties of Phases in the MAS
System

Phase	$\Delta H^0_{f,970}$, kJ mol^{-1}	S^0_{970}, J mol^{-1}K^{-1}	V^0_{970}, J bar^{-1}
Beta Phase (Mg$_2$SiO$_4$)	-34.0	268.3	4.166
Enstatite (CEn)	-62.05	380.6	6.220
Enstatite (hEn)	-66.04	388.15	6.438
Enstatite (1En)	-71.42	383.91	6.389
Enstatite (OEn)	-69.5	386.2	6.400
Enstatite (PEn)	-60.63	393.72	6.720
Forsterite	-64.0	275.0	4.450
Ilmenite (MgSiO$_3$)	17.25	184.5	2.765
Ilmenite (Al$_2$O$_3$)	45.9	174.9	2.435
Majorite	1.84	746.05	11.760
Mg-Tschermak Px	-6.85	379.9	6.050
Periclase	0	79.3	1.141
Perovskite (MgSiO$_3$)	105.75	191.4	2.435
Perovskite (Al$_2$O$_3$)	138.1	182.8	2.105
Pyrope	-82.35	768.4	11.600
Spinel (Mg$_2$SiO$_4$)	-23.3	260.7	4.046
Spinel (MgAl$_2$O$_4$)	-24.75	266.7	4.100
Stishovite	32.95	99.5	1.554

are most often determined at 970 K. A higher reference temperature is also closer to the experimental temperatures of the phase equilibrium studies; this minimizes discrepancies caused by the simplified treatment. Because of these discrepancies the parameters in Table 2 are not meant to replace the measured thermochemical values but rather to serve as simple means for calculating the phase relations in the MAS system and potentially in more complex systems. However, a comparison between the parameters in Table 2 and the measured thermochemical values is useful in evaluating the effects of the simplified treatment and identifying potential problems, either with the phase equilibria or the measured properties, from anomalously large discrepancies.

The thermodynamic properties of the low-pressure enstatite polymorphs were taken from Gasparik [1990b]. The enthalpies of formation from oxides of the remaining phases were calculated from the parameters derived in this study. Most of the calculated enthalpies are in good agreement with the measured values. The value for orthoenstatite is an average of three calorimetric values of Kiseleva et al. [1979], Chatillon-Colinet et al. [1983], and Brousse et al. [1984]. The value for forsterite is within uncertainties of the measured values of -64.4 kJ mol^{-1} by Torgesen and Sahama [1948] and -62.6 kJ mol^{-1} by Charlu et al. [1975]. Other values reported by Charlu et al. [1975] are also in good agreement: -84.6 kJ mol^{-1} for pyrope and -22.5 kJ mol^{-1} for MgAl$_2$O$_4$ spinel. The enthalpy of the beta phase is based on the measurements by Akaogi et al. [1984], while the enthalpy of Mg$_2$SiO$_4$ spinel is consistent with the upper limit of their measurements (6.8 ± 3.8 kJ mol^{-1} for $\Delta H(8)$). The enthalpy of majorite closely agrees with the value of 6 kJ mol^{-1} obtained from a linear extrapolation of the enthalpies of enstatite-pyrope garnets measured by Akaogi et al. [1987]. The value for ilmenite can be compared with 24.3 kJ mol^{-1} obtained from the measurements of Ashida et al. [1988]. However, the value for perovskite is higher than 75.4 kJ mol^{-1} based on the measurements by Ito et al. [1990].

The entropies in Table 2 were calculated to minimize discrepancies with the thermochemical measurements summarized by Robie et al. [1978] and Berman and Brown [1985]. The entropies agree to 1 J mol^{-1} K^{-1} for low

clinoenstatite, orthoenstatite, and periclase. The entropy for forsterite is 4 J mol^{-1} K^{-1} higher and for pyrope and MgAl$_2$O$_4$ spinel is 7 J mol^{-1} K^{-1} higher than the thermochemical data. The discrepancies could be explained by a disorder of magnesium and aluminum between the tetrahedral and octahedral sites in spinel [Hafner and Laves, 1961] and by a positional disorder of magnesium in the cubic subsites in pyrope [Zemann and Zemann, 1961; Hofmeister and Chopelas, 1991].

The volume data are most likely to show the discrepancies resulting from the simplified treatment. Particularly, the volumes of the high-pressure phases can not represent the true volumes at 970 K and 1 bar because they are based on the volume differences calculated at the corresponding high pressures using the Murnaghan equation [Gasparik, 1990a]. However, the volumes of the low-pressure phases are close to the measured values (adjusted for thermal expansion) because the pressure effect at corresponding low pressures is small. The unit-cell volumes of orthoenstatite and forsterite correspond to the measured values and serve as a reference. Good agreement was obtained for pyrope and MgAl$_2$O$_4$ spinel.

CONCLUSION

New experimental data along the enstatite-pyrope solidus allowed us to complete the phase diagram for the enstatite-pyrope join at very high pressures. The observed phase relations were closely reproduced with an internally consistent set of parameters. The emphasis was on providing a simple and practical tool for calculating the phase relations. Once the basic phase relations are understood, it is much easier to apply a thermodynamically more rigorous approach to reproduce these phase relations. Despite the simplified thermodynamic treatment, the obtained parameters are in a good agreement with the measured thermochemical values.

REFERENCES

Akaogi, M., and S. Akimoto, Pyroxene-garnet solid-solution equilibria in the system Mg$_4$Si$_4$O$_{12}$-Mg$_3$Al$_2$Si$_3$O$_{12}$ and Fe$_4$Si$_4$O$_{12}$-Fe$_3$Al$_2$Si$_3$O$_{12}$ at high pressures and temperatures, *Phys. Earth Planet. Inter.*, 15, 90-106, 1977.

Akaogi, M., N. L. Ross, P. McMillan, and A. Navrotsky, The Mg$_2$SiO$_4$ polymorphs (olivine, modified spinel and spinel)— Thermodynamic properties from oxide melt solution calorimetry, phase relations, and models of lattice vibrations, *Am. Mineral.*, 69, 499-512, 1984.

Akaogi, M., A. Navrotsky, T. Yagi, and S. Akimoto, Pyroxene-garnet transformation: Thermochemistry and elasticity of garnet solid solutions, and application to a pyrolite mantle, in *High-Pressure Research in Mineral Physics*, edited by M. H. Manghnani and Y. Syono, pp. 251-260, Terrapub, Tokyo, 1987.

Angel, R. J., L. W. Finger, R. M. Hazen, M. Kanzaki, D. J. Weidner, R. C. Liebermann, and D. R. Veblen, Structure and twinning of single-crystal MgSiO$_3$ garnet synthesized at 17 GPa and 1800°C, *Am. Mineral.*, 74, 509-512, 1989.

Ashida, T., S. Kume, E. Ito, and A. Navrotsky, MgSiO$_3$ ilmenite: Heat capacity, thermal expansivity, and enthalpy of transformation, *Phys. Chem. Miner.*, 16, 239-245, 1988.

Berman, R. G., and T. H. Brown, Heat capacity of minerals in the system Na$_2$O-K$_2$O-CaO-MgO-FeO-Fe$_2$O$_3$-Al$_2$O$_3$-SiO$_2$-TiO$_2$-H$_2$O-CO$_2$: Representation, estimation, and high temperature extrapolation, *Contrib. Mineral. Petrol.*, *89*, 168–183, 1985.

Boyd, F. R., and J. L. England, The system enstatite-pyrope, *Year Book Carnegie Inst. Washington*, *63*, 157–161, 1964.

Boyd, F. R., J. L. England, and B. T. C. Davis, Effects of pressure on the melting and polymorphism of enstatite, MgSiO$_3$, *J. Geophys. Res.*, *69*, 2101–2109, 1964.

Brousse, C., R. C. Newton, and O. J. Kleppa, Enthalpy of formation of forsterite, enstatite, akermanite, monticellite and merwinite at 1073 K determined by alkali borate solution calorimetry, *Geochim. Cosmochim. Acta*, *48*, 1081–1088, 1984.

Charlu, T. V., R. C. Newton, and O. J. Kleppa, Enthalpies of formation at 970 K of compounds in the system MgO-Al$_2$O$_3$-SiO$_2$ from high temperature solution calorimetry, *Geochim. Cosmochim. Acta*, *39*, 1487–1497, 1975.

Chatillon-Colinet, C., R. C. Newton, D. Perkins, and O. J. Kleppa, Thermochemistry of (Fe^{2+}, Mg)SiO$_3$ orthopyroxene, *Geochim. Cosmochim. Acta*, *47*, 1597–1603, 1983.

Chen, C.-H., and D. C. Presnall, The system Mg$_2$SiO$_4$-SiO$_2$ at pressures up to 25 kilobars, *Am. Mineral.*, *60*, 398–406, 1975.

Danckwerth, P. A., and R. C. Newton, Experimental determination of the spinel peridotite to garnet peridotite reaction in the system MgO-Al$_2$O$_3$-SiO$_2$ in the range 900°–1100°C and Al$_2$O$_3$ isopleths of enstatite in the spinel field, *Contrib. Mineral. Petrol.*, *66*, 189–201, 1978.

Gasparik, T., Transformation of enstatite-diopside-jadeite pyroxenes to garnet, *Contrib. Mineral. Petrol.*, *102*, 389–405, 1989.

Gasparik, T., Phase relations in the transition zone, *J. Geophys. Res.*, *95*, 15751–15769, 1990a.

Gasparik, T., A thermodynamic model for the enstatite-diopside join, *Am. Mineral.*, *75*, 1080–1091, 1990b.

Gasparik, T., Enstatite-jadeite join and its role in the Earth's mantle, *Contrib. Mineral. Petrol.*, *111*, 283–298, 1992.

Gasparik, T., and R. C. Newton, The reversed alumina contents of orthopyroxene in equilibrium with spinel and forsterite in the system MgO-Al$_2$O$_3$-SiO$_2$, *Contrib. Mineral. Petrol.*, *85*, 186–196, 1984.

Hafner, S., and F. Laves, Ordnung/Unordnung und Ultrarotabsorption III. Die Systeme MgAl$_2$O$_4$-Al$_2$O$_3$ und MgAl$_2$O$_4$-LiAl$_5$O$_8$, *Z. Kristallogr. 115*, 321–330, 1961.

Haselton, H. T., Calorimetry of synthetic pyrope-grossular garnets and calculated stability relations, Ph.D. thesis, 98 pp., Univ. of Chicago, Chicago, Ill., 1979.

Hatch, D. M., and S. Ghose, Symmetry analysis of the phase transition and twinning in MgSiO$_3$ garnet: Implications to mantle mineralogy, *Am. Mineral.*, *74*, 1221–1224, 1989.

Herzberg, C., and T. Gasparik, Garnet and pyroxenes in the mantle: A test of the majorite fractionation hypothesis, *J. Geophys. Res.*, *96*, 16,263–16,274, 1991.

Hofmeister, A. M., and A. Chopelas, Thermodynamic properties of pyrope and grossular from vibrational spectroscopy, *Am. Mineral.*, *76*, 880–891, 1991.

Howell, D. A., B. L. Phillips, R. J. Kirkpatrick, and T. Gasparik, Investigation of cation-ordering in majorites using ^{29}Si NMR spectroscopy, *Eos Trans. AGU*, *71*, 1666, 1990.

Ito, E., and E. Takahashi, Postspinel transformations in the system Mg$_2$SiO$_4$-Fe$_2$SiO$_4$ and some geophysical implications, *J. Geophys. Res.*, *94*, 10,637–10,646, 1989.

Ito, E., M. Akaogi, L. Topor, and A. Navrotsky, Negative pressure-temperature slopes for reactions forming MgSiO$_3$ perovskite from calorimetry, *Science*, *249*, 1275–1278, 1990.

Kanzaki, M., Ultrahigh-pressure phase relations in the system

Mg$_4$Si$_4$O$_{12}$-Mg$_3$Al$_2$Si$_3$O$_{12}$, *Phys. Earth Planet. Inter.*, *49*, 168–175, 1987.

Kato, T., and M. Kumazawa, Garnet phase of MgSiO$_3$ filling the pyroxene-ilmenite gap at very high temperature, *Nature*, *316*, 803–805, 1985.

Katsura, T., and E. Ito, The system Mg$_2$SiO$_4$-Fe$_2$SiO$_4$ at high pressures and temperatures: Precise determination of stabilities of olivine, modified spinel, and spinel, *J. Geophys. Res.*, *94*, 15,663–15,670, 1989.

Kiseleva, I. A., L. P. Ogorodova, L. P. Topor, and O. G. Chigareva, Thermochemical studies of CaO-MgO-SiO$_2$ system (in Russian), *Geokhimiya*, 1979, 1821–1825, 1979.

Liu, L., The system enstatite-pyrope at high pressures and temperatures and the mineralogy of the Earth's mantle, *Earth Planet. Sci. Lett.*, *36*, 237–245, 1977.

McMillan, P., M. Akaogi, E. Ohtani, Q. Williams, R. Nieman, and R. Sato, Cation disorder in garnets along the Mg$_3$Al$_2$Si$_3$O$_{12}$-Mg$_4$Si$_4$O$_{12}$ join: An infrared, Raman and NMR study, *Phys. Chem. Miner.*, *16*, 428–435, 1989.

Pacalo, R. E. G., and T. Gasparik, Reversals of the orthoenstatite-clinoenstatite transition at high pressures and high temperatures, *J. Geophys. Res.*, *95*, 15,853–15,858, 1990.

Perkins, D., T. J. B. Holland, and R. C. Newton, The Al$_2$O$_3$ contents of enstatite in equilibrium with garnet in the system MgO-Al$_2$O$_3$-SiO$_2$ at 15-40 kbar and 900°–1,600°C, *Contrib. Mineral. Petrol.*, *78*, 99–109, 1981.

Presnall, D. C., and T. Gasparik, Melting of enstatite from 10 to 16.5 GPa, *Eos Trans. AGU*, *70*, 483, 1989.

Presnall, D. C., and T. Gasparik, Melting of enstatite (MgSiO$_3$) from 10 to 16.5 GPa and the forsterite (Mg$_2$SiO$_4$)–majorite (MgSiO$_3$) eutectic at 16.5 GPa: Implications for the origin of the mantle, *J. Geophys. Res.*, *95*, 15,771–15,777, 1990.

Prewitt, C. T., and A. W. Sleight, Garnet-like structures of high-pressure cadmium germanate and calcium germanate, *Science*, *163*, 386–387, 1969.

Ringwood, A. E., The pyroxene-garnet transformation in the earth's mantle, *Earth Planet. Sci. Lett.*, *2*, 255–263, 1967.

Robie, R. A., B. S. Hemingway, J. R. Fisher, Thermodynamic properties of minerals and related substances at 298.15 K and 1 bar (10^5 pascals) pressure and at higher temperatures, *U.S. Geol. Surv. Bull.*, *1452*, 456 pp., 1978.

Sawamoto, H., Phase diagram of MgSiO$_3$ at pressures up to 24 GPa and temperatures up to 2200°C: Phase stability and properties of tetragonal garnet, in *High-Pressure Research in Mineral Physics*, edited by M. H. Manghnani and Y. Syono, pp. 209–219, Terrapub, Tokyo, 1987.

Torgesen, D. R., and T. G. Sahama, A hydrofluoric acid solution calorimeter and the determinations of the heats of formation of Mg$_2$SiO$_4$, MgSiO$_3$, and CaSiO$_3$, *J. Am. Chem. Soc.*, *70*, 2156–2160, 1948.

Wang, Y., T. Gasparik, and R. C. Liebermann, Modulated microstructure in MgSiO$_3$ garnet, *Eos Trans. AGU*, *72*(17), Spring Meeting Suppl., 146, 1991.

Zemann, A., and J. Zemann, Verfeinerung der Kristallstruktur von synthetischen Pyrop, Mg$_3$Al$_2$(SiO$_4$)$_3$, *Acta Crystallogr. 14*, 835–837, 1961.

T. Gasparik, SUNY Stony Brook, Department of Earth and Space Sciences, Stony Brook, NY 11794.